Journal of Clinical Monitoring and Computing (2009) 23:323–332
DOI: 10.1007/s10877-009-9200-1

COMPARISON OF TWO IN VIVO MICROSCOPY TECHNIQUES TO VISUALIZE ALVEOLAR MECHANICS

Johannes Bickenbach, MD[1], Rolf Dembinski, MD[1], Michael Czaplik, MD[2], Sven Meissner, MEng[3], Arata Tabuchi, MD, PhD[7], Michael Mertens, MSc, PhD[7], Lila Knels, MD[8], Wolfgang Schroeder, PhD[4], Paolo Pelosi, MD, PhD[5], Edmund Koch, MSc, PhD[3], Wolfgang M. Kuebler, MD, PhD[7], Rolf Rossaint, MD, PhD[1,2] and Ralf Kuhlen, MD, PhD[6]

Bickenbach J, Dembinski R, Czaplik M, Meissner S, Tabuchi A, Mertens M, Knels L, Schroeder W, Pelosi P, Koch E, Kuebler WM, Rossaint R, Kuhlen R. Comparison of two in vivo microscopy techniques to visualize alveolar mechanics.
J Clin Monit Comput 2009; 23:323–332

ABSTRACT. Objective. In conventional in vivo microscopy, a three dimensional illustration of tissue is lacking. Concerning the microscopic analysis of the pulmonary alveolar network, surgical preparation of the thorax and fixation of the lung is required to place the microscope's objective. These effects may have influence on the mechanical behaviour of alveoli. Relatively new methods exist for in vivo microscopy being less invasive and enabling an observation without fixation of the lung. The aim of this study was to compare a fibered confocal laser scanning microscopy (FCLSM) with optical coherence tomography (OCT) in a mouse and a rabbit model. Moreover, FCLSM was also used endoscopically in the rabbit model. **Methods.** Smallest possible thoracic windows were excised at the lower margin of the upper right lung lobe and an interpleural catheter inserted before re-coverage with a transparent membrane foil. The OCT-scanner was positioned by a motor driven translation stage. The imaging was gated to endinspiratory plateau. For CLSM, Fluorescein 0.1% was given into the central venous streak line. The confocal probe with a diameter of 650 μm was carefully positioned at the very same lung region. Images were directly recorded real-time and the observed region qualitatively compared with FD-OCT images. Additionally, in the rabbit model, CLSM was used endoscopically under bronchoscopic sight control. In a post-processing analysis, images taken were analyzed and compared by using an ''air index'' (AI). **Results.** In the mouse model, the very same region could be re-identified with both techniques. Concerning alveolar shape and size, qualitatively comparable images could be gained. The AI was 40.5% for the OCT and 40.1% for the CLSM images. In the rabbit, even an endoscopic view on alveoli was possible. Likewise AI was 43.2% for CLSM through the thoracic window and 43.6% from endoscopically. For the OCT an AI of 44.6% was analysed in the rabbit model. **Conclusions.** Both FD-OCT and CLSM provide high-resolution images of alveolar structure giving depth information that is beneficial to conventional microscopy. CLSM also facilitates endoscopic view on alveoli being well comparable to images gained through a thoracic window.

KEY WORDS. in vivo microscopy, alveolar mechanics, mechanical ventilation.

From the [1]Department of Surgical Intensive Care, University Hospital RWTH Aachen, Pauwelsstr. 30, 52074 Aachen, Germany; [2]Department of Anaesthesiology, University Hospital RWTH Aachen, Aachen, Germany; [3]Clinical Sensoring and Monitoring, Medical Faculty, TU Dresden, Dresden, Germany; [4]Institute of Aerodynamics, RWTH Aachen, Aachen, Germany; [5]Department of Environment, Health and Safety, University of Insubria, Varese, Italy; [6]Department of Intensive Care Medicine, Helios Hospital Berlin Buch, Berlin, Germany; [7]Institute of Physiology, Charité, Universitaetsmedizin Berlin, Berlin, Germany; [8]Department of Anesthesiology, University Hospital Dresden, Dresden, Germany.

Received 6 March 2009. Accepted for publication 18 August 2009.

Address correspondence to J. Bickenbach, Department of Surgical Intensive Care, University Hospital RWTH Aachen, Pauwelsstr. 30, 52074 Aachen, Germany.
E-mail: jbickenbach@ukaachen.de

INTRODUCTION

The microscopic view on the behaviour of the expansion of the alveolar network may be of potential interest to better understand the effects of alveolar mechanics on the

global pulmonary function during spontaneous and mechanical ventilation.

Although dynamical changes in pulmonary alveolar structure during artificial ventilation may be observed by in vivo microscopy alveolar mechanics has not been fully elucidated yet. Different techniques have been proposed to directly visualize the mechanical behaviour of distinct alveolar regions [1–6].

A substantial number of existing studies is using a two-dimensional in vivo video microscopy describing alveolar mechanics in a porcine and in a rat model [1–6]. Briefly this technique consists of a superficial view on alveoli after fixation by a glass plate and suction.

Interestingly, different alveolar regions could be identified according to their different mechanical character when changing ventilatory settings. Various acute lung injury (ALI) models [6, 7] were found to differently affect regional alveolar mechanics [6, 7]. In our opinion, although extremely innovative, this method suffers from several limitations, which may affect its accuracy and precision: (a) it gives information about a limited parenchymal area, (b) it needs the surgical opening of the thorax. First, this makes this technique not applicable in humans; secondly, the transpulmonary pressures are modified, being part of the lung open to atmosphere, thus affecting regional lung mechanics at end expiration and inspiration.

Ideally, a visualization technique to investigate alveolar mechanics should be used not only in vivo, but also in real time, be non invasive and hopefully clinically applicable in humans, an extensive alveolar area should be investigated and finally fixation should be avoided to exclude artificial behaviour of alveoli.

The optical coherence tomography (OCT) [8] has been proposed as an alternative for alveoli imaging through a thoracic window. It is a relatively new non-invasive imaging technique providing high-resolution structural information based on an Interferometer of short coherent near infrared (NIR) light [8]. OCT is qualified for imaging lung parenchyma [11] yielding full three dimensional information comparable to conventional intravital microscopy [12].

The spectral domain variant Fourier domain OCT (FD-OCT) [9, 10] allows examining alveolar mechanics during mechanical ventilation [11]. It gives depth information from the first subsurface 500 μm of highly scattering tissue with a resolution better than 10 μm. As a reference method, convectional dark field microscopy (DFM) is often parallely used with FD-OCT, particularly to re-identify specific lung regions.

The fibered confocal laser scanning microscopy (CLSM) is a relatively new application device that provides a clear, high resolution in-focus image of a living sample [13]. The microscope's objective is replaced by a flexible fiberoptic miniprobe of less than 1 mm in diameter.

In the present study we tested a minimally invasive fibered confocal microscopy system that also allows endoscopic view on alveoli and enables real-time dynamic observation of different lung regions. This innovative method was only used in a previous study with different clinical purposes [14]. In addition, the imaging quality was compared with conventional dark field microscopy (DFM) and FDOCT both in a mouse and a rabbit model.

We hypothesized that the described techniques and the resulting alveolar structures can be well compared.

Moreover, in the rabbit model, we hypothesized that alveolar mechanics can be equally observed either endobronchially or through a thoracic window.

METHODS

Mouse model

Male Balb/c mice of 23–30 g bodyweight (bw) (Charles River Wiga GmbH, Sulzfeld, Germany, $n = 2$) were used. All experiments were performed in accordance with the ''Guide for the Care and Use of Laboratory Animals'' (Institute of Laboratory Animal Resources, 7th edition 1996). The study was approved by the animal care and use committee of the local government authorities.

Surgical preparation

Mice were anesthetized by intraperitoneal injection of medetomidine (0.5 mg/kg bw, Domitor®, Dr. E. Graeub AG, Basel, Switzerland), fentanyl (0.05 mg/kg bw, JanssenCilag, Neuss, Germany), and midazolam (5 mg/kg bw, Dormicum®, Roche, Basel, Switzerland) as previously described [15]. Anesthetic depth was evaluated regularly by limb-withdrawal to paw pinch, and anesthesia was maintained by repetitive injections of half of the dose necessary for initial anesthesia induction every 30–60 min.

Anesthetized mice were placed in supine position on a heating pad and body temperature was maintained via a feedback coupled rectal thermoprobe at 37.0°C. Two catheters (Portex® FineBore Polythene Tubing, 0.28 mm ID/0.61 mm OD, Smiths Medical International Ltd., Keene, NH) were inserted into the right external jugular vein for the injection of drugs and fluorescent dyes, and for continuous fluid replacement (0.2 ml/h of 6% hydroxyethylstarch; HES 6% 200/0,5, Fresenius, Bad Homburg, Germany).

Following catheter placement, mice were tracheotomised, intubated with a polyethylene tube (Portex®

FineBore Polythene Tubing, 0.58 mm ID/0.96 mm OD; Smiths Medical International Ltd.) and positioned in left decubitus position. Animals were ventilated with room air at 100 breaths/min and end-inspiratory and end-expiratory pressures of 11 and 1 cm H_2O, respectively (Animal Respirator Compact 4600-Series, TSE Systems, Bad Homburg, Germany). The skin over the right rib cage was removed and the medial and caudal ends of the underlying muscles were dissected to expose ribs and intercostal muscles of the right anterior-lateral thoracic wall. By partial resection of the 3rd to 5th rib, a 7–10 mm circular window was excised in the centre of which the lower margin of the upper right lung lobe was exposed. Special care was taken to avoid any mechanical contact with the intact lung surface. After placement of a transdiaphragmal catheter (Portex® FineBore Polythene Tubing, 0.58 mm ID/0.96 mm OD; Smiths Medical International Ltd.) into the right intrapleural space, the window was covered with a transparent polyvinylidene membrane (New Kure Wrap, Kureha Co., Tokyo, Japan) and tightly sealed with B-cyanoacrylate glue (Pattex; Henkel, Duesseldorf, Germany). Intrathoracic air was removed via the intrapleural catheter, thus establishing direct coupling of the lung surface to the transparent window membrane. After air removal, the intrathoracic pressure was reconstituted at −3 mmHg and recorded continuously thereafter (DasyLab 32; DasyLab).

Rabbit model

Briefly, female rabbits (New Zealand White, $n = 2$) weighing 3 kg were anesthetized with ketamine 50 mg/kg and xylazine hydrochloride 4 mg/kg after cannulation of an ear vein. Anesthetic depth was evaluated regularly by limb-withdrawal to paw pinch, and anesthesia was maintained by repetitive injections of half of the dose necessary for initial anesthesia induction every 30–60 min.

Tracheotomy was performed with a custom made suction catheter. After skin preparation and removal, the medial and caudal ends of the underlying muscles were dissected to expose ribs and intercostal muscles of the right anterior-lateral thoracic wall. A 10–15 mm circular window was excised in the center of which the lower margin of the upper right lung lobe was exposed. After insertion of an interpleural catheter, the window was again covered with a transparent polyvinylidene membrane as described for the mouse model.

Animals were ventilated volume controlled (8 ml/kg bw) with room air and a respiratory rate of 30 breaths/min. Inspiratory peak pressure was limited to 12 mbar, PEEP was set at 1 mbar (KTR-4 small animal ventilator, Harvard Apparatus, Holliston, United States).

Dark field microscopy and FD-optical coherence tomography

A schematic description of dark field microscopy and FD-optical coherence tomography within the measurement set up is briefly illustrated (Figure 1). As light source a superluminescent diode (Superlum Russia) with a centre wavelength of 830 nm, a full width half maximum of 50 nm and an optical power of 1 mW were used. The light is transmitted to the scanner head by fibre optics. All components of the interferometer are integrated into the scanner head. The measurement beam is splitted in sample and reference beam by a beam splitter cube. In order to scan the probe surface the sample beam is deflected by two electrical controlled galvanometer scanners (Cambridge Technologies).

The backscattered light from the sample and the reference light reflected by a mirror are superimposed by the beam splitter cube. The emerged interference signal is transmitted into a spectrometer by fibre optics, where it is spectrally resolved. The interference spectrum is detected by a CCD (charge coupled device) line detector with an A-scan rate of 12 kHz. By using a fast Fourier transformation the spectrum intensity is transformed into the corresponding depth information.

A 2 MB Pixel USB camera with a frame rate of 20 fps for this resolution is adapted by microscopy optics in the scanner head for dark field microscopy (DFM). Thus it is possible to acquire simultaneous OCT and DFM images of the same investigation area. The illumination for DFM is realised by a ring light consisting of 12 ultra high white light emitting diodes in front of the scanner head. Furthermore the camera provides an excellent orientation on the probe surface. For positioning the scanner head is mounted on a three axis translation stage.

Confocal laser scanning microscopy

For confocal microscopy, an exogenous staining was used. Fluorescein 0.1% was applied into the central venous line right before the beginning of microscopy. The confocal probe (CellVizio®, S-1500 ProFlex™, Mauna Kea Technologies, Paris, France) with a diameter of 650 μm produces images from a layer of 0 to 15 μm in axial resolution, with a lateral resolution of 5 μm, and a field-of-view up to 600 μm in diameter. The probe needs to be in direct contact with tissue. The laser scanning unit (LSU) provides both its illumination and detection capabilities. It performs a complete raster scanning of the entire fibre bundle 12 times every second by means of rapid oscillating mirrors that illuminate each fibre and collect the corresponding fluorescent light signal. In short, this produces a systematic X–Y optical view of the tissue being explored

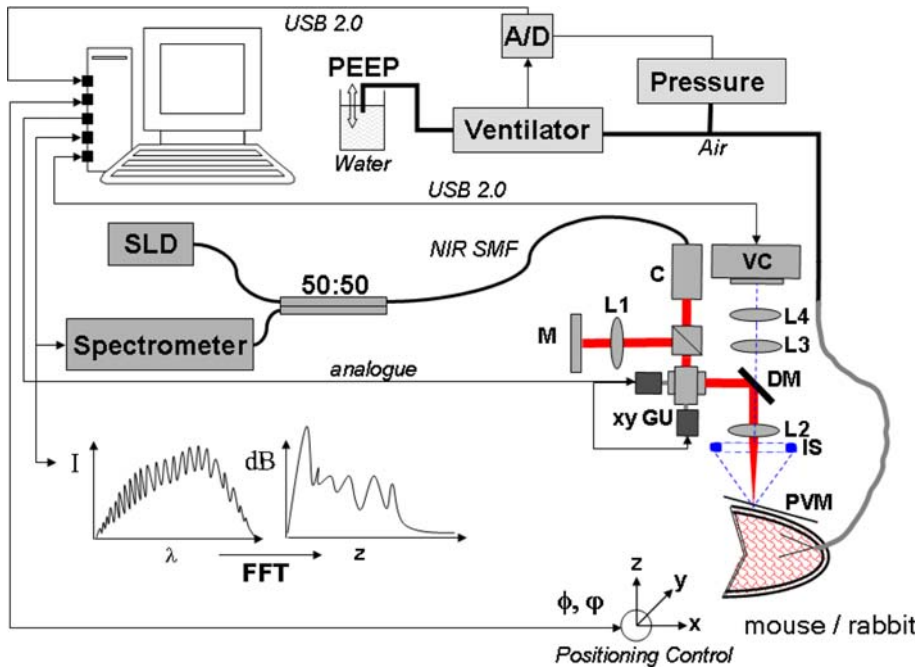

Fig. 1. Measurement setup of the gated OCT and DFM imaging of the in vivo subpleural lung parenchyma. Abbreviations: λ wave length, z depth, SLD Superluminescent diode, NIR SMF near infrared single mode fibre, M reference mirror, L1 reference lens, C collimator, xy GU xy deflection galvanometer unit, DM dielectric mirror, L2 object lens, IS illumination, PVM polyvinylchloride membrane, L3/L4 microscope lens, VC video camera, A/D analogue digital converter.

in real-time. The LSU used operates at 488 excitation wavelength. The excitation strength can be readily adapted to the flourophore concentration in order to make the most out of the available fluorescence signal.

For gaining images through the thoracic window, the probe was carefully positioned on the foil guided by a motor driven translation stage.

Moreover, in the rabbit model, an other probe was applied giving a more three dimensional image of alveolar structure due to a higher depth of observation (60 μm) but hence a smaller field of view (200 μm) (CellVizio®, Type MiniO, Mauna Kea Technologies, Paris, France). Due to the diameter, it could not be used in the smaller mouse model.

For endoscopic imaging in the rabbit model, the probe was introduced under bronchoscopic sight control into the right middle lobe as far as possible. For imaging alveoli, the probe was further advanced carefully until an adequate signalling could be recorded.

The LSU interfaces directly with an Apple computer (Mac OS X, Version 10.4.8) installed with an imaging software package (Image Cell 3.6.2, Mauna Kea Technologies, France) that provides instrument control, real-time image reconstruction and analysis, calibration and data storage capabilities.

According to striking landmarks (e.g., vessels, boundaries between lung lobes), the very same lung region was selected with any technique.

Alveolar shape was qualitatively analyzed and their size was measured. Moreover, angles of alveolar structures and of capillary junctions were consulted.

Study protocol

After preparation, DFM was firstly initialized as this technique was used as a reference method. Its objective was positioned on the surface of the lung parenchyma. FD-OCT imaging acquisition from the very same lung region was taken thereafter. The OCT-scanner was positioned by a motor driven translation stage. The imaging was gated to endinspiratory plateau. Three-dimensional OCT image stacks were acquired by progressively scanning an area of 1.2×1.2 mm with 300×300 spectra and on-the-fly-saving to hard disc. The spectral data was further processed offline into grey value image stacks representing the logarithmized Fourier amplitudes.

After having finished imaging acquisition by FD-OCT, Fluorescein was given into the central venous streak line. For CLSM, the confocal probe was again carefully positioned at the very same lung region. Images were directly

recorded in real-time and the observed region qualitatively compared with DFM and FD-OCT images. Data was recorded for at least 1 min.

In the rabbit model endoscopic imaging was performed thereafter. After adequate signalling, data was recorded for at least 1 min.

After this process, images were qualitatively compared and regions showing the same alveolar structure were re-identified. After completion of imaging, the animals were sacrificed and the lungs were examined to exclude any parenchymal damage.

Post processing analysis

Quantification of the images was performed with NI Vision (National Instruments, Munich, Germany). After adequate windowing, the resulting layers of the examined region were analysed with the NI Vision Assistant. A script with the following logic arrays was developed:

1. Standardization of the gray scale values on the basis of histogram analysis.
2. Air-filled compartments were identified by setting empiric threshold values for pre-defined gray scales allowing adequate quantification.
3. Calculation of an ''air index'' (ratio between amount of air and tissue within the observed region of interest) for each layer in order to compare the different imaging techniques independent from the size of the examined region. The air index (AI) allows quantitative comparison of the imaging techniques.

This procedure was conducted for both the CLSM and the OCT technique. Moreover a quantitative comparison of endoscopic and external CLSM images was carried out.

RESULTS

All animals survived the entire study period. Examination of all animals by a veterinary surgeon prior to the study showed no signs of infection or pulmonary diseases. Post-mortem examination of the lungs did not reveal any sign of pulmonary disease or damage of the pulmonary parenchyma.

Both in the FD-OCT and in the CLSM images, light structures are assigned to lung parenchyma whereas dark, black structures are related to air filled structures, i.e., alveoli and/or alveolar ducts.

Mouse model

Comparison between DFM, FD-OCT and CLSM acquired through a thoracic window

Concerning DFM, imaging of alveolar structure could be obtained from different lung regions. For comparison with the other imaging techniques, specific anatomic structures were chosen to identify comparable images. One of the images is shown representatively in Figure 2.

For each OCT volume scan one corresponding DFM image was identified. The FD-OCT images show

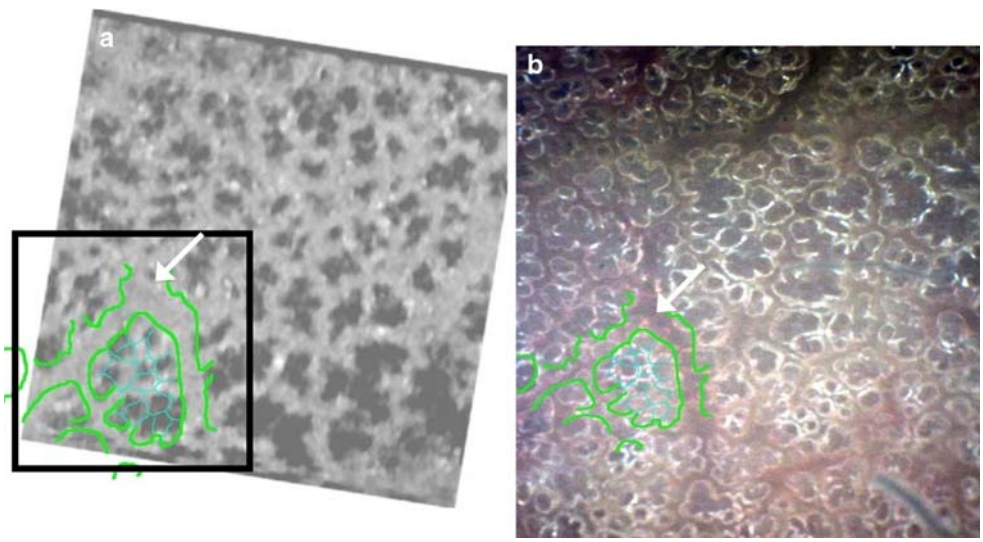

Fig. 2. Demonstration of FD-OCT image stacks in the mouse model (a, left) with 1004 × 1552 μm (width × height). White arrow shows angle of a marked arteriole. The structure of the vessel and alveoli is traced. Black square shows area that was enlarged and where alveolar size was measured. DFM (b, right) acquired in analogy with FD-OCT. White arrow again shows angle of a marked arteriole. The structure of the vessel and alveoli is traced.

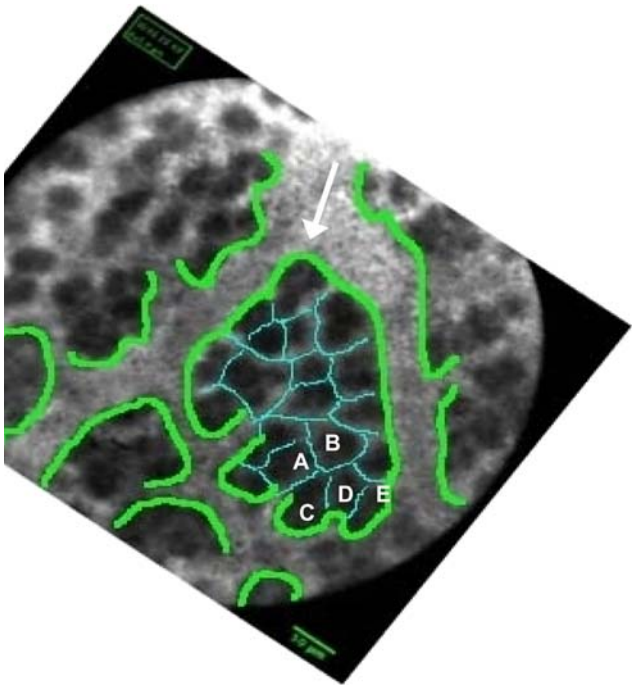

Fig. 3. Demonstration of CLSM with a field of view of 600 μm in diameter. White arrow shows angle of a marked arteriole. The structure of the vessels and alveoli is traced. Alveoli were characterized (A–E) for exemplary measurement of alveolar size in one animal.

reproducible quality concerning shape and character of alveolar structure when compared to DFM. Remarkably, the coexistence of single delimitable alveoli and alveolar ducts seem to demonstrate an imagination of the three dimensional alveolar network.

With CLSM, the exact same region of the lung could be identified by the run of vessels. The imaging was assessable after intravenous staining with fluorescein (Figure 3). Again, comparable structure can be demonstrated. Due to re-identification of the very same region and a same distribution and size of alveoli (Table 1) both methods seem well comparable in the mouse model.

Post processing image analysis

Concerning quantification of the imaging techniques, an AI of 40, 5% for the OCT and 40, 1% for the CLSM images could be measured. According images can be seen in Figure 4.

Rabbit model

Comparison between DFM, FD-OCT and CLSM images acquired through a thoracic window

Again, alveolar structure could be examined within both imaging techniques. However, identification of the very same lung region was not feasible in this model. For FD-OCT, alveolar structure is representatively demonstrated in Figure 5.

Table 1. Alveolar size of selected alveoli of one region of interest of one animal measured as an example for FD-OCT and CLSM in a mouse model

	FD-OCT	CLSM
A[μm^2]	2144	2178
B[μm^2]	1888	1736
C[μm^2]	1616	1648
D[μm^2]	1328	1270
E[μm^2]	848	921

CLSM again necessitated an i.v. staining with fluorescein right before image acquisition. In vivo imaging of alveolar structure could be demonstrated for different lung regions.

Figure 6 demonstrates an exemplary region measured with two different probes; the right image shows view on alveolar structure with a probe giving a more three dimensional image of alveolar structure due to a higher depth of observation.

Comparison between endoscopic CLSM and CLSM through a thoracic window

Moreover, endoscopic in vivo imaging was performed under bronchoscopic sight control. The right middle lobe could be identified and the probe was further introduced until an adequate image could be gained (Figure 7).

Qualitatively as well as concerning shape and size of alveolar structure, both imaging techniques seem well comparable. Strikingly the run of vessels can be seen in a different manner: from the endoscopic perspective and due to the optical path of the laser, vessels are gated longitudinally whereas a vertical gate is displayed in the CLSM images through a thoracic window.

For showing alveolar dynamics during artificial ventilation, a video sequence of endoscopic in vivo CLSM can be viewed as supplementary material.

Post processing image analysis

With the NI Vision Assistant endoscopic CLSM and CLSM through a thoracic window as well as OCT-images were measured resulting in an AI of 43.2, 43.6 and 44.6%, respectively. Corresponding images are depicted in Figure 8.

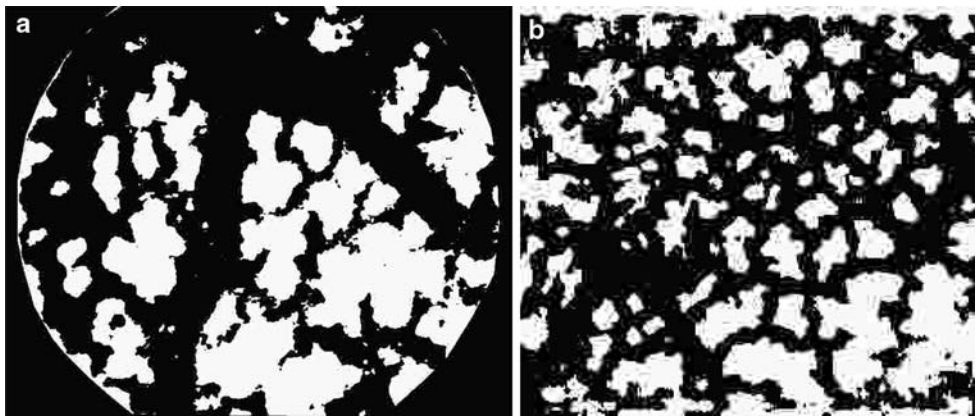

Fig. 4. Quantification of both imaging techniques resulting in an AI of 40.1% for the CLSM (a) and 40.5% for the FD-OCT (b).

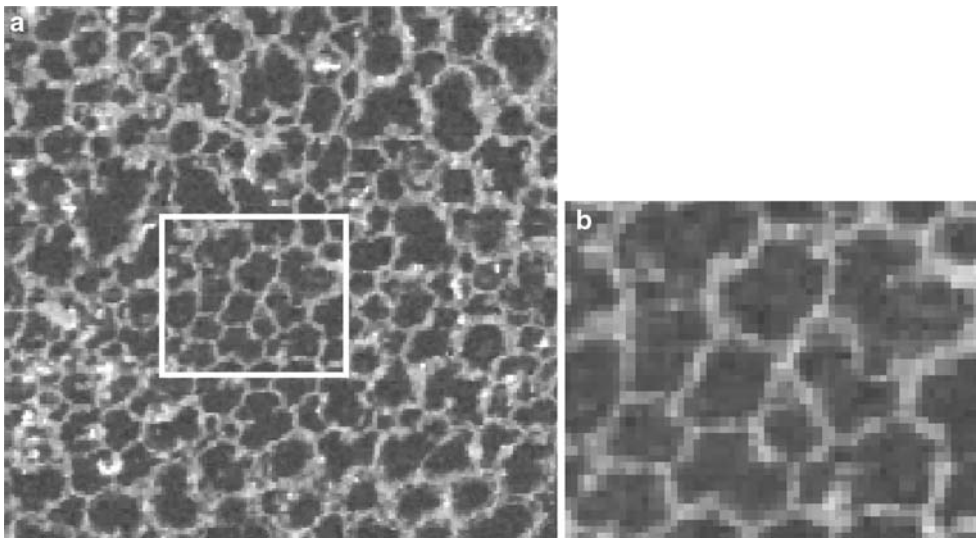

Fig. 5. Demonstration of in vivo FD-OCT image stacks with 1004 × 1552 μm (width × height) in the rabbit model (a). White square shows area that was enlarged and where alveolar size was measured (b).

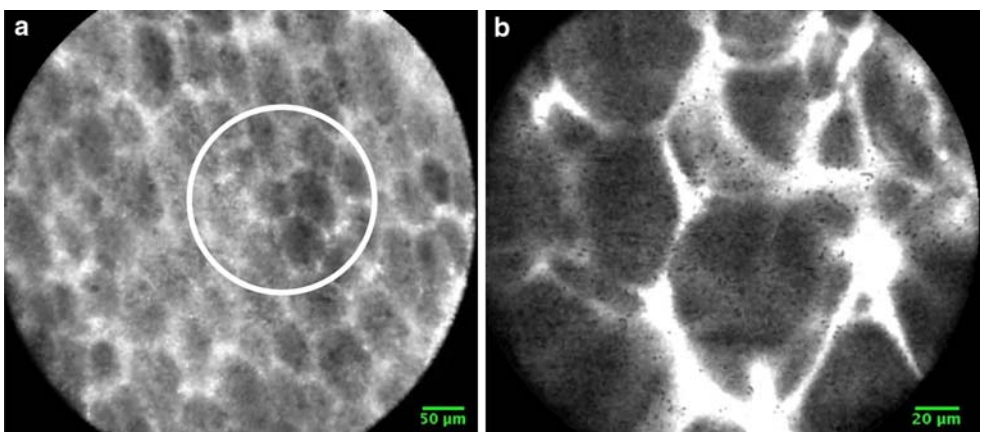

Fig. 6. Demonstration of CLSM with the S1500-probe (a, left, field of view of 600 μm in diameter) in a rabbit model. White circle identifies the region obtained with the MiniO probe (b, right, field of view 200 μm in diameter) giving a more three dimensional image of the alveolar network.

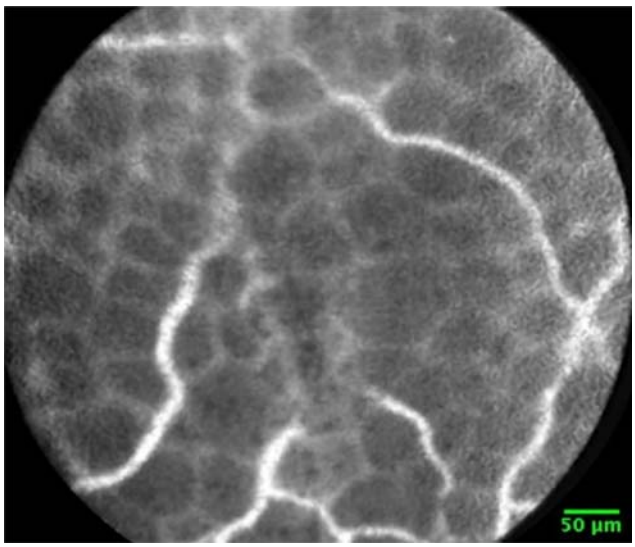

Fig. 7. Endoscopic in vivo CLSM in a rabbit model.

DISCUSSION

Imaging alveolar mechanics demands a method that provides high-resolution images giving depth-information and that can be used in vivo. This feasibility study aimed to compare two relatively new methods, namely Fourier domain optical coherence tomography (FD-OCT) and confocal laser scanning microscopy (CLSM) used through a thoracic window hypothesizing that the allegorized alveolar structures can be qualitatively and quantitatively compared in different small animal models.

Moreover, in the rabbit model, CLSM was also utilized endoscopically hypothesizing that alveolar mechanics can be equally observed either endobronchially or through a thoracic window.

Firstly, we demonstrated that the resolution of FD-OCT and CLSM images is sufficient to show individual alveoli. Both techniques reveal shape information of alveolar structure. Both FD-OCT and CLSM allow

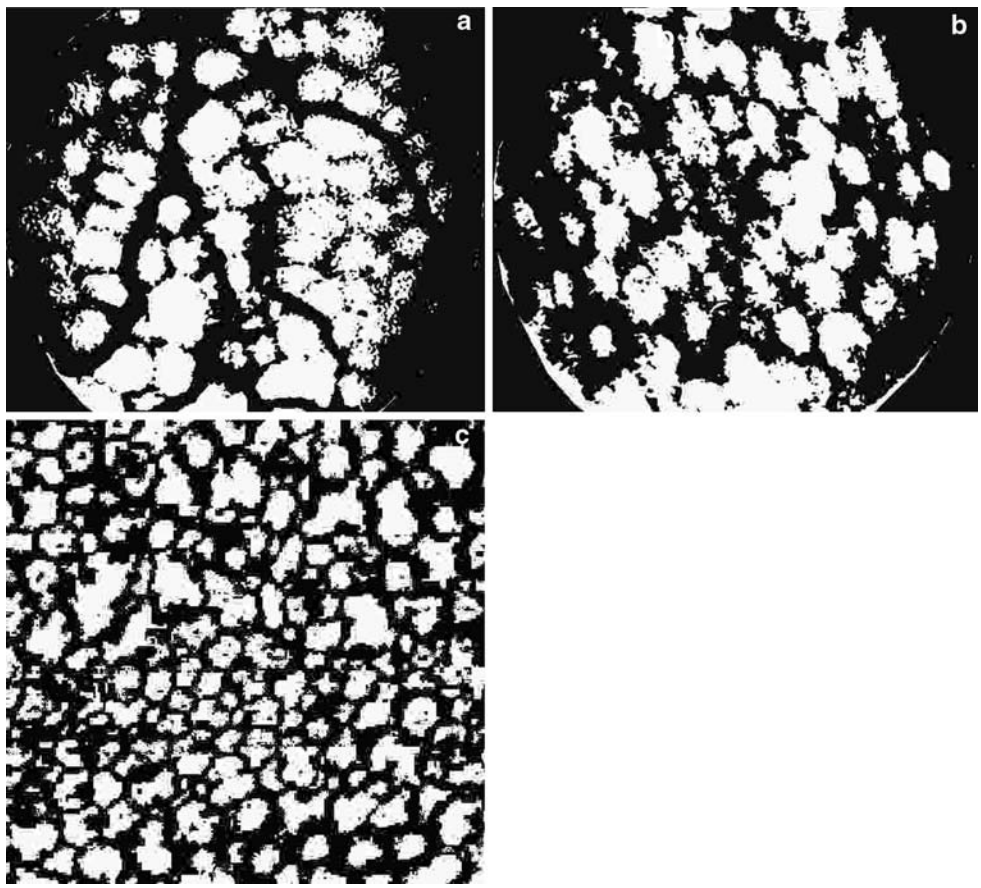

Fig. 8. Resulting images after post-processing analysis with the NI Vision Assistant. AI was 43.2% for the endoscopic CLSM (a), 43.6% for CLSM through thoracic window (b) and 44.6% for the OCT (c).

analysis of alveolar structure as well as an unambiguous comparison in the mouse model concerning the quality of images. However, in the rabbit model, identification of a very same lung region did not succeed. The technique of FD-OCT in an in vivo rabbit model seems limited due to the movement of the lung so that the scanning procedure of FO-OCT is more difficult. Nevertheless, even in the rabbit model, imaging of alveolar structure can be well demonstrated with both techniques.

Secondly, imaging with CLSM yielded an endoscopic view on alveoli in the rabbit model demonstrating the same alveolar structure than from ''outside''. Of course, comparing the images, it needs to be taken into account that a different optical path scans the tissue leading to a different display of the vessels. However, as shown in the post-processing analysis, the AI is comparable.

Additionally, as seen in the video sequence, dynamical alveolar mechanics can be observed and therefore, endoscopic in vivo CLSM could be used to systematically examine different lung regions at the microscopic alveolar level. This may give further information about the mechanical behaviour of the alveolar network during artificial ventilation. Furthermore, this technique offers a less invasive approach to the alveolar network. It allows examination of the lung without opening the thorax and thus without influencing regional lung mechanics and transpulmonary pressures.

In older studies, the examination of alveolar dynamics during different ventilatory patterns was restricted to microscopic images of subpleural alveoli after fixation with a cover glass and suction [1–5]. In our study, fixation was not necessary and the thoracic window was closed after preparation to simulate a closed chest.

Compared to conventional microscopy, both FD-OCT and CLSM provide a further insight into alveolar mechanics due to more depth information as it could be seen with the CLSM as well as with the FD-OCT. This further knowledge may prevent from misinterpretation of two-dimensional imaging as observed by conventional microscopy. Potential movement artefacts could lead to aberrant analysis of changes of alveolar size emerging from cutting alveoli on another level only. Other than in conventional microscopy, the expansion of alveoli into depth during artificial ventilation can be observed.

Although the depth information of these techniques is advantageous over conventional microscopy, it is still limited to subpleural alveoli which not obligatorily represent alveolar mechanics of the whole lung. As a matter of fact, the penetration depth of FD-OCT is limited to scattering of the probe light within the lung tissue. Hence this is a principal limitation of the OCT technique in imaging aerated lungs.

For the CLSM, the MiniO-probe, which could be used in the rabbit model, has a depth of observation of 60 μm. Depth information is restricted to the first three layers of subpleural alveoli. Additionally, the field of view is limited to 200 μm so that the region of interest and therefore the amount of alveoli is further reduced. However, imaging with this probe may at least give an idea about the three dimensional structure of the alveolar network.

The endoscopic approach could resolve this technical limitation allowing to analyse not only alveoli approachable from ''outside'' but alveolar mechanics from every region of the lung.

Moreover it has to be taken into account that only small animals were analysed in this study. A conclusion to mechanical behaviour of alveoli in bigger animals or human beings can only be assumable. Besides, this first evaluation was only done in healthy but not in injured lungs. It would be interesting to further examine alveolar dynamics also in experimental lung injury and while using different ventilatory patterns. In this first application, the focus was laid on evaluating two relatively new techniques. Therefore, further examination needs to be done to also analyse alveolar mechanics in injured lungs.

The fact that no statistical analysis could be included due to the small number of animals is another limitation. Nevertheless, the main focal point was on qualitatively comparing the two techniques and this seems feasible. Concerning quantitation, the implementation of an AI could be a helpful tool to numerically compare the techniques. The shown results may indicate a good correlation, however, this needs to be further deepened in further studies.

In conclusion, it can be stated that both FD-OCT and CLSM are imaging techniques that provide high-resolution images of alveolar structure giving depth information that is beneficial to conventional microscopy in a mouse and in a rabbit model. Moreover, the methods can be clearly compared in an in vivo mouse model. Additionally, although limited in analysing the very same lung region, both imaging techniques can be well compared in an in vivo rabbit model.

Regarding CLSM, this imaging technique also facilitates endoscopic view on alveoli being well comparable to images gained through a thoracic window.

Therefore, both techniques may help to further investigate in vivo alveolar mechanics gaining further insight into the complex three dimensional structure of the network. Both techniques may be helpful devices used for clinical application. Particularly in intensive care settings were patients need to be mechanically ventilated due to respiratory insufficiency, they may help to better understand mechanical behaviour of alveolar structure

during artificial ventilation and their potential effects on the global pulmonary function.

The study was supported by research grant KU 1372/5-1 from the "Deutsche Forschungsgesellschaft (DFG)".

REFERENCES

1. Schiller HJ, Steinberg J, Halter J, McCann U, DaSilva M, Gatto LA, et al. Alveolar inflation during generation of a quasi-static pressure/volume curve in the acutely injured lung. Crit Care Med 2003; 31(4): 1126–1133.
2. Halter JM, Steinberg JM, Schiller HJ, DaSilva M, Gatto LA, Landas S, et al. (Positive end-expiratory pressure after a recruitment maneuver prevents both alveolar collapse and recruitment/derecruitment. Am J Respir Crit Care Med 2003; 167(12): 1620–1626.
3. Steinberg J, Schiller HJ, Halter JM, Gatto LA, DaSilva M, Amato M, et al. Tidal volume increases do not affect alveolar mechanics in normal lung but cause alveolar overdistension and exacerbate alveolar instability after surfactant deactivation. Crit Care Med 2002; 30(12): 2675–2683.
4. Schiller HJ, McCann UG, Carney DE, Gatto LA, Steinberg JM, Nieman GF. Altered alveolar mechanics in the acutely injured lung. Crit Care Med 2001; 29(5): 1049–1055.
5. Halter JM, Steinberg JM, Gatto LA, Dirocco JD, Pavone LA, Schiller HJ, Albert S, Lee HM, Carney DE, Nieman GF. Effect of positive end-exspiratory pressure and tidal volume on alveolar instability-induced lung injury. Crit Care 2007; 11(1): R20.
6. Pavone LA, Albert S, Carney D, Gatto LA, Halter JM, Nieman GF. Injurious mechanical ventilation in the normal lung causes a progressive pathologic change in dynamic alveolar mechanics. Crit Care 2007; 11(3): R64.
7. DiRocco JD, Pavone LA, Carney DE, Lutz CJ, Gatto LA, Landas SK, Nieman GF. Dynamic alveolar mechanics in four models of lung injury. Intensive Care Med 2006; 32(1): 140–148.
8. Huang D, Swanson EA, Lin CP, Schuman JS, Stinson WG, Chang W, Hee MR, Flotte T, Gregory K, Puliatito CA, Fujimoto JG. Optical coherence tomography. Science 1991; 254: 1178–1181.
9. Häusler G, Lindner MW. Coherence radar and spectral radar—new tool for dermatological diagnosis. J Biomed Opt 1998; 3(1): 21–31.
10. Fercher AF, Hitzenberger CK, Kamp G, El-Zaiat SY. Measurement of intraocular distances by backscattering spectral interferometry. Opt Commun 1995; 117: 43–48.
11. Popp A, Wendel M, Knels L, Kocht T, Koch E. Imaging of the three-dimensional alveolar structure and the alveolar mechanics of a ventilated and perfused isolated rabbit lung with Fourier domain optical coherence tomography. J Biomed Opt 2006; 11(1): 014015 .
12. Carney D, DiRocco J, Nieman G. Dynamic alveolar mechanics and ventilator-induced lung injury. Crit Care Med 2005; 33: S122–S128.
13. Le Goualher G, Perchant A, Genet M, Cavé C, Viellerobe B, Bérier F, Abrat B, Ayache N. Towards optical biopsies with an integrated fibered confocal fluorescence microscope. In: Lecture notes in computer science. Vol. 3217(II). Berlin/Heidelberg: Springer; 2001; 761–768.
14. Thiberville L, Moreno-Swirc S, Vercauteren T, Peltier E, Cavé C, Bourg Heckly G. In vivo imaging of the bronchial wall microstructure using fibered confocal fluorescence microscopy. Am J Respir Crit Care Med 2007; 175(1): 22–23.
15. Tabuchi A, Mertens M, Kuppe H, Pries AR, Kuebler WM. Intravital microscopy of the murine pulmonary microcirculation. J Appl Physiol 2008; 104: 338–346.